Arab J. Nucl. Sci. Appl., Vol. 56, 2, 131-139 (2023)

Paper presented in the 10th African Conference on Research Reactor Safety, Operation & Utilization, Cairo (Egypt) 27 to 29 Nov. 2022, organized by the International Atomic Energy Agency in cooperation with the Egyptian Atomic Energy Authority

ISSN 1110-0451

Arab Journal of Nuclear Sciences and Applications

Web site: ajnsa.journals.ekb.eg

IAEA

Inspection of Some Components of the Nuclear Reactor TRICO II

L.P. Kaja Mukinay[1], D. Kadima Mutombo[1], C. Mujinga Kalonji[1], B. Mandungu Kiese[1], P. Kuba Ndomatezo[1], W. Lukibanza Lufumbwa[1], S. Ilunga Tshimbela[1], J. Muswema Lunguya[1], O. Shetonde Mihigo[2], D. Kabeya Ngalamulume[1]

(1) *Commissariat Général à l'Energie Atomique/Centre Régional d'Etudes Nucléaires de Kinshasa, B.P.868 Campus de l'Université de Kinshasa/République Démocratique du Congo*

(2) *Université de Kinshasa. Département de Chimie. Campus Universitaire de Kinshasa.*

ARTICLE INFO

Article history:

Received: 10th Nov. 2022

Accepted: 16th Jan. 2023

Keywords:

Non-destructive testing;

Visual inspection;

Ultrasonic Testin.

ABSTRACT

In order to restart the Research Reactor Trico II, nuclear components are inspected using two main Non-Destructive Testing (NDT) methods, namely Visual Inspection (VI) and Ultrasonic Testing (UT). Visual method was needed to inspect the TANK using underwater camera ARECONT VISION and the USB2.0 endoscope. Ultrasonic method was needed to inspect octagonal concrete structure using a flaw detector Proceq Pundit PL-200PE for uniformity and quality controls. The inspection showed that the reactor tank has not been degraded. Indeed, out of about one hundred photos taken with both underwater cameras, only two shows small degradations on the tank wall. One concerns the horizontal ring 1, which is not well sticked on the tank wall. The second concerns the vertical weld (CV1), which shows a visible spot on the weld due probably to dust accumulation. The biological protection layer of the octagonal concrete structure is not also degraded. The calculated concrete structure elasticity modulus is given by $G = 192\ 558{,}53 \pm 43811{,}93$ Mpa.

INTRODUCTION

Important works construction in industry presenting a considerable life-time is now possible due to material sciences evolution and industrial technical progress. It is well known that maintenance of industrial equipment prolongs its components life-time and operability. This is the case for nuclear research reactors and plants. It is also known that maintenance involves inspection methods. Generally, for components inspection, destructive methods are used. However, the latter are time consuming, expensive and necessitates to stop the industrial process in order to remove selected components for subsequent inspections. Non-destructive Testing (NDT) methods are now more used [1]. Indeed, they are very rapid, less expensive and, depending to components to be inspected, do not necessitate to stop the reactor.

As required by safety authorities, to restart its Research Reactor Trico II after an extended shut-down since 2005, in August 2021, the General Commission for Atomic Energy (GCAE)/ Regional Center for Nuclear Study of Kinshasa (RCNS-K) decided to make an inspection of Trico II to assess conditions for long-term future operation. Information for Periodic Safety Review (PSR) are available from the in-service inspections that contains a program of inspections for adequate safety in order to remediate deterioration and ageing issues and to replace outdated components [2,3].

To restart Trico II, for the Democratic Republic of the Congo (DRC) Safety Authorities, among inspections planned in the in-service inspections, the assessment of actual conditions of the reactor site were mandatory involving geophysics aspects namely

Corresponding author: kabeyadieudonne10@gmail.com
DOI: 10.21608/AJNSA.2023.172591.1676

soil stability due to buildings (soil compaction) and conditions of building themselves. Therefore, the present paper is devoted to one of inspections involved in the in-service inspections, namely the reactor tank inspection and, as said above, the assessment of the state of the reactor octagonal concrete structure. After discussions between NDT team and Trico II staff, among issues addressed by the latter, the NDT team have been challenged to retrieve two objects fallen in the tank bottom during maintenance operations. Note that several meetings were also organized between the Trico II Safety Committee (TSC) and the NDT team.

Two Non-Destructive Testing methods (NDT), namely the visual Inspection (VI) and the ultrasonic testing (UT), have been selected. The inspection of the Trico II tank was guided by the paper by J. Jerman [4]. Based on analyses of possible degradation processes, the visual inspection must permit to detect defects in all inner surface of the reactor tank wall, namely corrosions, mechanical deformations, visible cracks and other surface defects. A particular stress must be put on rings and welds. The ultrasonic testing was used to determine the state of octagonal concrete structure of Trico II.

I. MATERIAL AND METHODS

To meet the requirements of the above-mentioned analyses, the underwater camera ARECONT VISION, AV3100M 3megapixel IP-camera sensitive to 02 lux@F1.4 and the USB.2.0 endoscope, built-in 8,5mm diameter along with six LED lights and IP67 waterproof construct quality to give a closer view to inspect larger to tiny things found underwater, dark places, of wet areas easily. It can be moved within a range of 15 meters to examine objects effortlessly. Data were transferred and saved in AVI format on the laptop for further use (Fig.1).

The two cameras were used to inspect the internal part of the TRICO II tank wall. According to written procedures, rings, welds and tank wall parts inspected are named in order to be discriminated in the inspection report. All the selected pictures for the present work are given in the next section. Results interpretation is done according to ASME CODES [5]. The ultrasonic testing used the flaw detector Proceq Pundit PL-200PE for uniformity and quality controls of the reactor octagonal concrete structure. Recall that the latter is a heavy concrete constructed in 1972. For pulse echo mode, each couple of detectors of the flaw detector Proceq Pundit PL-200PE was tested in site using its dry coupling in plastic (fig.2a) and calibrated using the corresponding dry coupling in plastic (Fig.2b).

a)

b)

Fig. (1): Photos a) and b) shows the underwater camera ARECONT VISION and endoscope USB.2.0, respectively.

a)

b)

Fig. (2): a) and b) show the display and the flaw detector Proceq Pundit PL-200PE with the plastic coupling for testing probes and the calibration of the pulse echo through transmission mode, respectively.

a)

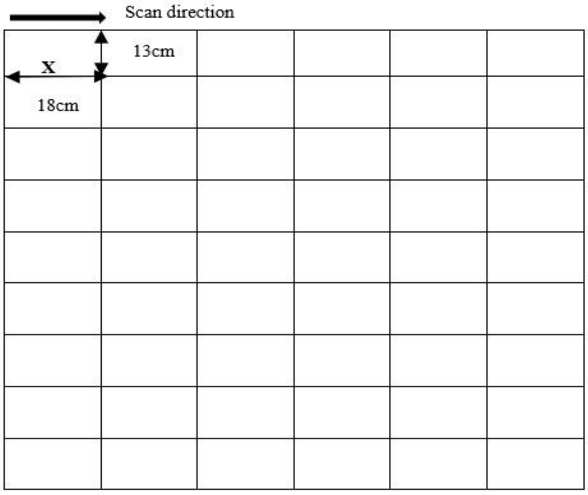

b)

Fig. (3): Photo 3a) and scheme 3b) show the octagonal concrete structure of Trico II and the mesh defined for B-scan, respectively. The scanning begins by the grid X.

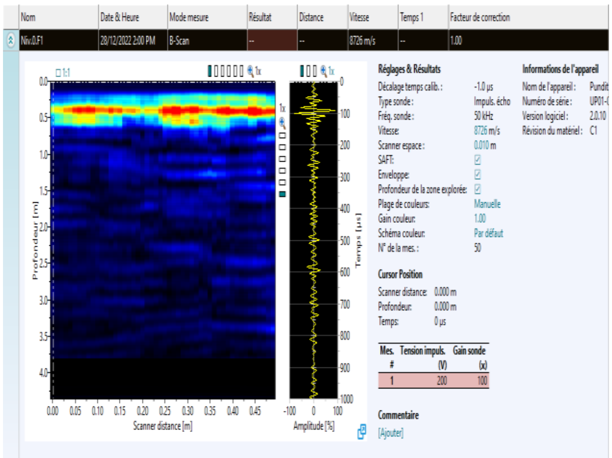

a)

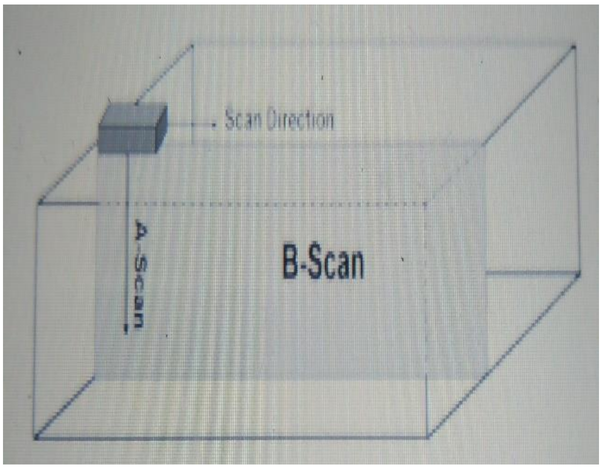

b)

Fig. (4) a) and b) respectively, show an example of the ultrasonic result on the face 1 (Niv.0.F1) and the process of the B-Scan on a test piece.

Provided the fact that the inspection is the first since 1972, the written procedure required 100 percent of inspection extension. Therefore, a mesh was defined in each face of the concrete structure. Figure 3a shows the photo of the octagonal concrete structure of Trico II. Given the equipment dimensions: (18x13) $cm^2 = 234\ cm^2$, each grid of 234 cm^2 is defined in the mesh to be a point of ultrasonic measurement (fig. 3b). The result of each face is the average of three measurements. The flaw detector Proceq Pundit PL-200PE display gives a left area for B-scan (The transversal section of the structure that represents the different densities of the structure by different colors) and a right area for A-scan (The pulse-echo method that represents the amplitude of the echo in the structure). For a measurement, the detector is placed perpendicularly to the face. Note that the A-scan permits to determine the longitudinal velocity v_l in the concrete of a known width. B-scan is obtained by changing the grid in the scan direction. The example given in figure 4a represents a UT measurement on face 1 (Niv.0.F1), whereas the figure 4b explains the UT measurement process on a test piece.

II. RESULTS

About 100 photos have been taken through visual inspections and are available in Trico II archives. Only photos that present degradations are selected in this paper. An observation along with remedial actions to be taken are also given. However, as illustration, figure 5 shows a photo of the following good welds in T, namely the horizontal weld (CH2) and the vertical weld (CV2). Figures 6 and 7 concern photos with small degradations. Figure 8 show photos with objects fallen in the tank bottom. Figures. 9a and b show respectively the vertical section of the Trico II and the measurement in pulse-echo mode on one grid.

Results of UT measurements of the octagonal concrete structure are given in table 1. They were collected according to the succession of faces as defined in the photo of figure 3a. Faces 1, 2, 3, 4, 5, 6, 7 and 8 are in the bottom. Face $1'$, $2'$, $3'$, $4'$, $5'$, $6'$, $7'$ and $8'$ are in the top. Faces 2 and $2'$ are opposite to the thermal column face in the anti-clockwise sense. Each face contains a layer of unknown material of different colors (red-yelow). According to one of Trico II radioprotection officers, it represents a protective biological shielding inserted in each face during the concrete structure construction. It is the object of a next NDT work on Trico II. The corresponding depths are reported in table 1 in the fifth column. The correction factor represents a systematic error on A-scan and B-scan respectively given by the flaw detector Proceq Pundit PL-200PE incorporated software (fig.4a).

Fig. (5): Photo of good welds in T: horizontal weld (CH2) and vertical weld (CV2). The photo was taken with the underwater endoscope USB 2.0.

Table (1): The above table reports the ultrasonic longitudinal and transversal velocities measurements on each face. The second column contains values of each face width. In third and fourth columns, v_{la} and v_{Ta}, respectively, represent averages of the three values of the measured longitudinal and transversal velocities v_l and v_T on each face. The fifth column reports the unknown material measured width of each face.

	Width (m)	Longitudinal velocity v_l (m/s)	Transversal velocity v_T (m/s)	Un. Mat. Measured width (m)	Correction factor	E-Modulus MPa	Poisson coefficient
Reference block	0.70	2756	1515,8		0.1	192558,53 $\pm$ 43811,93	0.28
Face1	2.277	8826 9294 8060 v_{la} =8726.67	4854,3 5111,7 4433 v_{Ta} = 4799,67	0.34	0.1		
Face 2	2.277	8060 8060 8809 v_{la} =8309.67	4433 4433 4844,95 v_{Ta} = 4570,32	0.62	0.1		
Face 3	2.277	8074 8808 8046 v_{la} =8309.67	4440,7 4844,4 4425,3 v_{Ta} = 4570,13	0.34	0.1		
Face 4	2.277	8826 9731 8809 v_{la} =9122	4854,3 5352,05 4844,95 v_{Ta} = 5017,1	0.25	0.1		
Face 5	2.277	8826 8089 8893 v_{la} =8602.67	4854,3 4448,95 4891,15 v_{Ta} = 4731,47	0.35	0.1		
Face 6	2.277	8060 8060 8060 v_{la} =8060	4433 4433 4433 v_{Ta} = 4433	0.22	0.1		
Face 7	2.277	8046 8060 8826 v_{la} =8310.67	4425,3 4433 4854,3 v_{Ta} = 4570,87	0.24	0.1		
Face 8	2.277	8626 8626 8626 v_{la} =8626	4744,3 4744,3 4744,3 v_{Ta} = 4744,3	0.25	0.1		
Face 1’	0.83	9071 9022 9071 v_{la} =9054.67	4989,05 4962,1 4989,05 v_{Ta} = 4980,07	0.25	0.1		

Face 2'	0.83	7477 7444 7411 v_{la} =7444	4112,35 4094,2 4076,05 v_{Ta} = 4094,2	0.25	0.1
Face 3'	0.83	8384 8384 8973 v_{la} =8580.33	4611,2 4611,2 4935,15 v_{Ta} = 4719,19	0.42	0.1
Face 4'	0.83	8737 8137 9379 v_{la} =8764	4805,35 4475,35 5158,45 v_{Ta} = 4813,05	0.29	0.1
Face 5'	0.83	8925 8877 9822 v_{la} =9208	4908,75 4882,35 5402,1 v_{Ta} = 5064,4	0.28	0.1
Face 6'	0.83	8034 8300 8973 v_{la} =8435.67	4418,7 4565 4935,15 v_{Ta} = 4639,62	0.30	0.1
Face 7'	0.83	7037 7615 7094 v_{la} =7248.67	3870,35 4188,25 3901,7 v_{Ta} = 3986,77	0.26	0.1
Face 8'	0.83	7155 8973 7064 v_{la} =7730.67	3935,25 4935,15 3885,2 v_{Ta} = 4251,87	0.31	0.1

Note that flaw detector Proceq Pundit PL-200PE software also has the possibility to compute the Poisson coefficient ν and the elasticity modulus G of the concrete by using following formula:

$$\nu = \frac{v_L^2 - 2v_T^2}{2(v_L^2 - v_T^2)} \quad (1)$$

and $$G = \frac{v_L^2.\rho.(1+\nu).(1-2\nu)}{(1-\nu)} \quad (2)$$

The symbol v_T represents the ultrasonic wave transversal velocity. It is defined by $v_T \cong 0{,}55.v_l$. Symbol ρ is the concrete volumic mass. The Poisson coefficient is given by ν = 0.28. It is very close to the theoretical value, that is 0.3. The longitudinal velocity v_l of the octagonal concrete structure is the average of all v_{La} reported in table 1. Thus, $v_l = (8408{,}335 \pm 989)\frac{m}{s}$. In the same way, $v_T = (4624{,}16 \pm 538{,}83)\frac{m}{s}$. Thus, the elasticity module calculated from v_l is given by: $G = (192\ 558{,}53 \pm 43811{,}93)$ Mpa.

III. DISCUSSION

- The photo of figure 6 was taken with the underwater USB.2.0 endoscope.
- Observation: Its dimensions are not uniform. This indicates that the horizontal ring 1 is not well sticked on the tank wall.
- Remedial action: The horizontal ring 1 must be well sticked on the tank wall.
- The photo of figure 7 was taken with the underwater USB.2.0 endoscope.
- Observation: The photo shows a visible spot on the weld, due probably to dust accumulation.

- Remedial action: A test of pressurized water can be done to verify the dust accumulation hypothesis.
- Photos of figure 8 was taken with the underwater camera ARECONT VISION.
- Observation 1: The first image indicates the presence of a fallen object in the tank bottom.
- Remedial action: An appropriate tool is conceived to remove it from the bottom.
- Observation 2: The second image indicates the presence of wires in the tank bottom.
- Remedial action: The above-mentioned tool will be used to remove them from the tank bottom.

For the octagonal concrete structure, velocity measurements for each face indicate, according to ref.[6], that the structure is not degraded. Indeed, $(8{,}408335 \pm 0{,}989)$ Km/s.$10^3 > 4{,}5$ Km/s.10^3. This value indicates that the concrete is excellent. B-scan of each face shows very small difference in densities that do not have a significant impact on concrete characteristics. All B-scan photos are available in the Trico II archives.

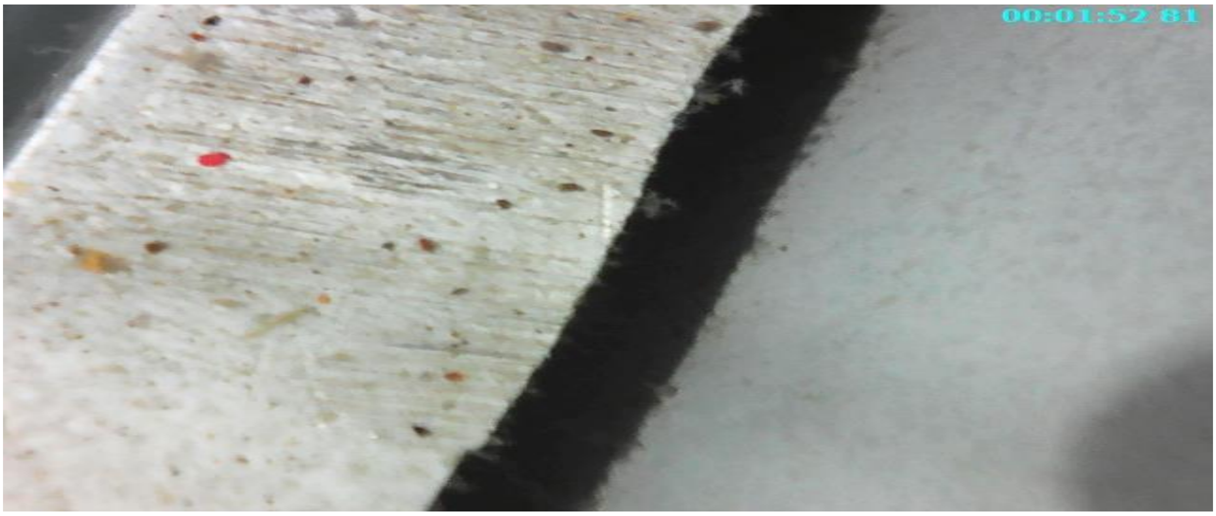

Fig. (6): The photo shows the Horizontal ring 1.

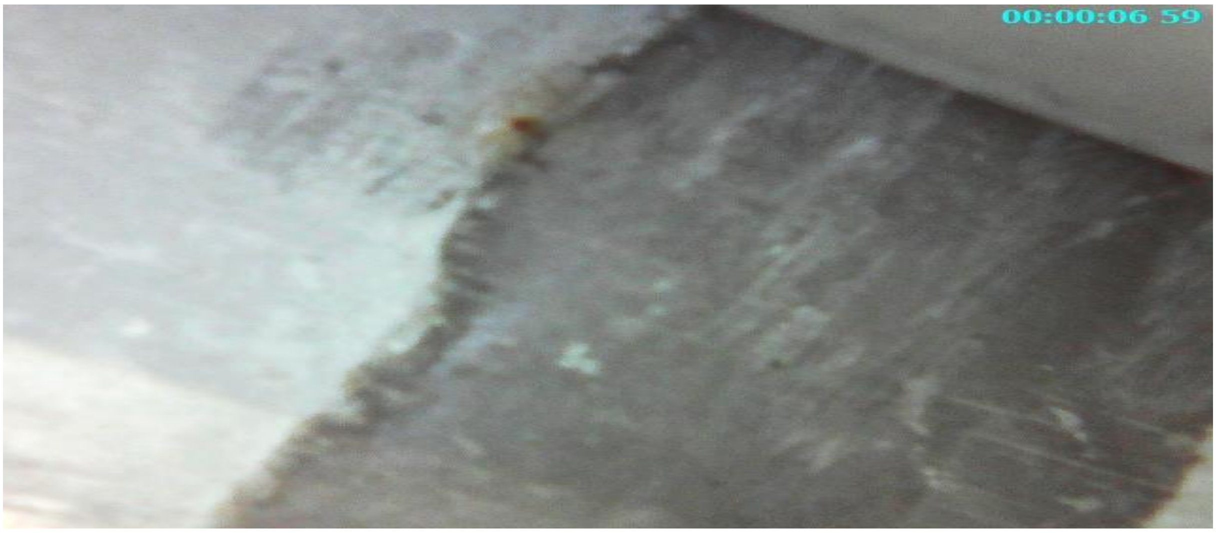

Fig. (7): The photo shows the Vertical weld (CV1)

Fig. (8): The two photos show locations of the two fallen objects in the tank bottom.

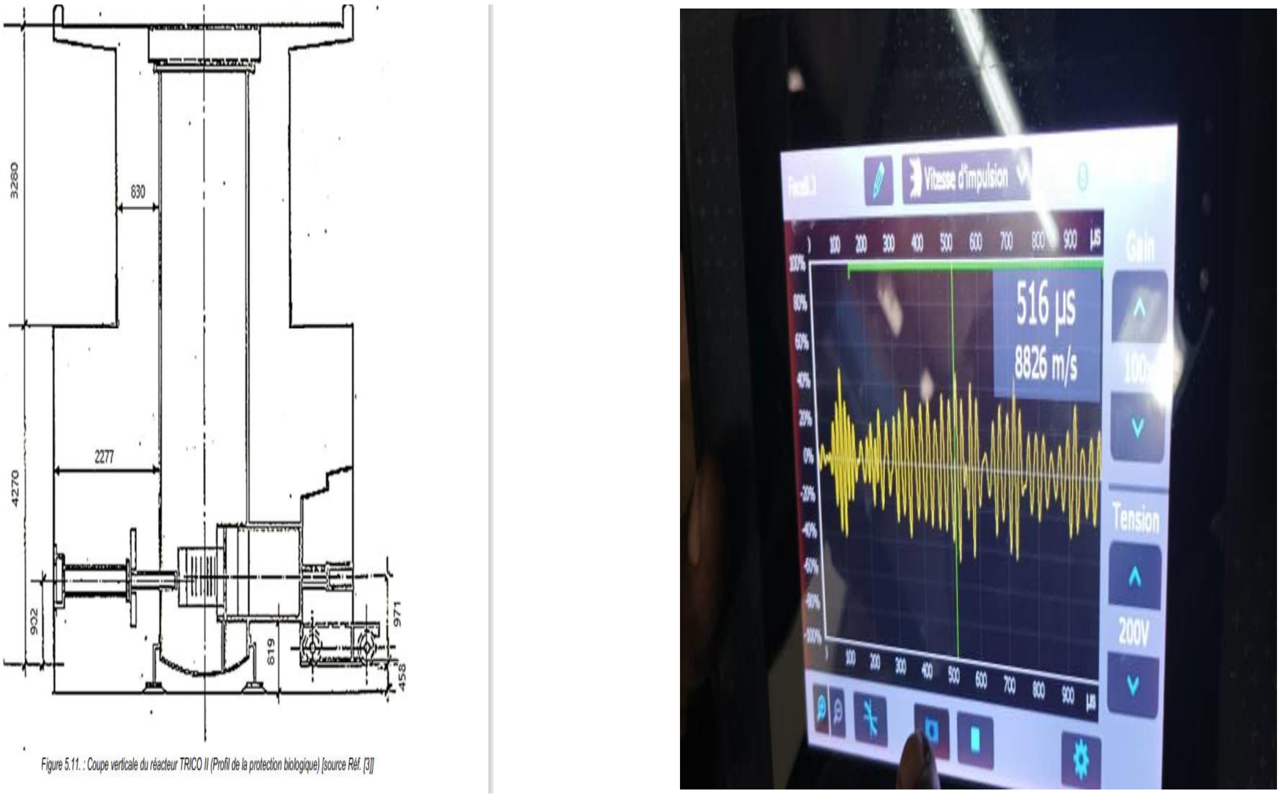

Fig. (9): Figures a) and b), respectively, show the vertical section of the Trico II and the measurement in pulse-echo mode on one grid.

IV. CONCLUSION

The main conclusion is that, apart from proposed remedial actions, the Trico II tank is not degraded and have a long-term operability. Locations of the two objects fallen in the tank bottom are determined and can be removed using the tool conceived for this purpose.

V. REFERENCES

[1] INTERNATIONAL ATOMIC ENERGY AGENCY, (2001) Application of non-destructive Testing and in-service inspection to research Reactors, IAEA-TECDOC-1263, IAEA, Vienna, 30-31

[2] INTERNATIONAL ATOMIC ENERGY AGENCY, (2006) Maintenance, Periodic Testing and Inspection

of Research Reactor, IAEA Safety Stantards Series No. NS-G-42, IAEA, Vienna, 10-15

[3] NITISWATI, S, et al., “Ageing management and effective utilization (Proc. Int. Conf. Sydney, 2007), IAEA, Vienna (2008) CD-ROM

[4] JERMANS, J. LESNJAK, A. SNOJ, L. SMODIS, B. “Inspection of the TRIGA Reactor Tank” (NENE Conf. Ljubljana, 2012)

[5] ASME B&PV Code Section XI, edition 2007.

[6] INTERNATIONAL ATOMIC ENERGY AGENCY, VIENNA, Guidebook on non-destructive testing of concrete structures IAEA, IAEA-TCS-17 ISSN 1018-5518, VIENNA, pp 103-110 (2002).